



Research article

Simultaneous spectrophotometric determination of Co (II) and Co (III) in acidic medium with partial least squares regression and artificial neural networks

Nausheen Yasin^{a,*}, Syed Mumtaz Danish Naqvi^a, Syed Mamnoon Akhter^b^a Department of Applied Chemistry and Chemical Technology, University of Karachi, Karachi, Pakistan^b Department of Applied Physics, University of Karachi, Karachi, Pakistan

ARTICLE INFO

Keywords:

Cobalt
Co (II)
Co (III)
Redox couple
Artificial neural network
Partial least squares regression
Multivariate analysis
UV-Visible spectroscopy

ABSTRACT

This study aims at the application of two chemometric techniques to visible spectra of acetic acid solutions of Co (II) and Co (III) for simultaneous determination thereof. Spectral data of 145 samples in the range of 400–700 nm were used to build the models. Partial least squares regression models were developed for which latent variables were determined using internal cross-validation with a leave-one-out strategy and 3 and 2 latent variables were selected for Co(II) and Co(III) based on root mean square error of cross-validation. For these models, root mean square errors of prediction were 1.16 and 0.536 mM and coefficients of determination were 0.975 and 0.892 for Co (II) and Co (III). As an alternate method, artificial neural networks consisting of three layers, with 10 neurons in hidden layer, were trained to model spectra and concentrations of cobalt species. Levenberg-Marquardt algorithm with feed-forward back-propagation learning resulted root mean square errors of prediction of 0.316 and 0.346 mM for Co (II) and Co (III) respectively and coefficients of determination were 0.996 and 0.988.

1. Introduction

According to a study, the carboxylates, typically acetates of cobalt in wet acetic acid, are the most extensively used homogeneous catalysts in the organic industry [1]. For more than a century, the redox couple Co (II)/Co (III) has been prepared in different ways and used per se where other catalysts stand flop due to selectivity problems or economic and environmental constraints [2,3]. Several modifications of this catalyst such as a combination with Mn and Br have also been suggested [4]. A free-radical chain mechanism governs such reaction networks, resulting in hydroperoxides as intermediate that may catalytically be decomposed in chain branching steps, in the presence of Co(III)/Co(II), generating free radicals for propagation [5,6]. The composition of Co(II)/Co(III) solution has a decisive influence on the process kinetics [7], however, simultaneous determination of both species of cobalt in acetic acid is quite challenging. Methods available so far include gravimetric analysis [8], chelation and solvent extraction [9], paper and thin layer chromatographic techniques [10–13], polarography [14], extractive [15] and non-extractive spectrophotometric methods [16,17] and atomic absorption spectroscopy [8,18]. These techniques may satisfactorily be applied with reasonable accuracy but the cost, operational complications, and laborious pretreatment or separation steps are some of the reasons hindering their routine use in laboratories with limited resources. Hence a simple method without any pre-treatment or separation step is much needed for compositional

* Corresponding author.

E-mail address: nyasin@uok.edu.pk (N. Yasin).

<https://doi.org/10.1016/j.heliyon.2024.e26373>

Received 21 July 2023; Received in revised form 18 December 2023; Accepted 12 February 2024

Available online 16 February 2024

2405-8440/Â© 2024 The Authors. Published by Elsevier Ltd. This is an open access article under the CC BY-NC-ND license (<http://creativecommons.org/licenses/by-nc-nd/4.0/>).

analysis of Co (II) and Co (III) solution in acetic acid.

Spectrophotometry combined with chemometric techniques such as multivariate data analysis is the most applicable, economical, and versatile analytical method for the quantitative analysis. Its potential applications are found in various fields such as environmental monitoring [19,20], quality control [21,22], process analytical technology [23,24], food and pharmaceutical analyses [25–27], data-driven process systems engineering [28,29], process optimization [30,31] and quantitative structure–analysis relationships [32]. The recent proliferation of chemometric algorithms such as partial least squares regression (PLS) and artificial neural networks (ANN) has boosted the use of spectrophotometry as a simple, rapid, and nondestructive method for the analysis of complex mixtures. There are several reports on multicomponent analysis in which PLS regression has been proved to be a simple and fast chemometric method to deal with highly collinear variables [27,32,33]. However, the nonlinearities in data could limit its applications. ANN is an alternate technique having the ability to learn by examples and to model linear as well as nonlinear relationships in data to build a global model [34–36]. These techniques are successfully applied for speciation analysis as well [37–39]. There are multiple reports in literature highlighting the application of chemometric tools for cobalt analysis in the presence of other metals [16,17,40,41] but the results are reported as total cobalt. To our knowledge, there has been no report on using such methods for the simultaneous determination of Co (II) and Co (III) in acetic acid medium.

The main goal of the present work is to extend the use of chemometric methods such as partial least squares (PLS) and artificial neural networks (ANNs) for the prediction of both Co (II) and Co (III) species simultaneously in acidic medium. The main difference in the present study and the previously published work is that simultaneous determination of both forms is without any tedious steps of separation or masking the species. The comparison of both models has also been presented using different statistical parameters.

2. Materials and methods

2.1. Reagents and solutions

Cobalt (II) acetate tetrahydrate (proanalysis) was purchased from Merck and used without any further purification. AnalR-grade potassium chlorate and potassium iodide were procured from BDH. Distilled water was used during experiments. The standard stock solution of sodium thiosulfate was prepared from an extra pure reagent from Seharlain. Lab reagent grade anhydrous sodium acetate and pure glacial acetic acid were acquired from Fluka and pure isopropyl alcohol was purchased from Sigma Aldrich.

2.2. Apparatus

All glassware of Pyrex Class A was used. An automatic pipette from Nichiryo was used for careful preparation of samples. Thermo circulator and hot plate stirrer from LabTech were used to maintain the reaction bath at a constant temperature. Titrations were precisely performed using an automatic burette (continuous E) from Vitlab (Germany). Spectra was collected by Shimadzu UV-1650 PC UV-Vis spectrophotometer equipped with a matched pair of 1-cm quartz cells.

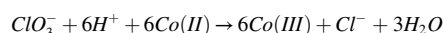
2.3. Software and data analysis

PLS-SIMPLS algorithm and computational programs for ANN were written in MATLAB (v. 6.5 for Windows). Intel Core i7-3770 3.4 GHz with Microsoft Windows 10 operating system was used to run all programs.

2.4. Sample preparation for spectral data

Training and test data sets for ANN and PLS model development were initially prepared by mixing different amounts of reactants in the laboratory.

A large data set of 145 samples of binary mixtures comprising Co (II) and Co (III) was used to model the quantitative relationship between the concentration of both redox species and their spectra. Since Co (III) acetate is not widely available commercially, that's why the solutions of redox couple were prepared by adopting a straightforward route of oxidizing cobalt (II) acetate in glacial acetic acid with a calculated amount of aqueous potassium chlorate according to the following reaction [42]:



Various amounts of 0.05 M Co (II) acetate were made to react with different volumes of 0.23 M potassium chlorate at 85 °C in glacial acetic acid to prepare a set of 145 samples in the laboratory for composition analysis and the resulting solutions were analyzed for Co (III) concentration by iodometric method. A plethora of aesthetically pleasing colors results from variations in the concentration of Co (II) and Co (III) from magenta to purplish brown to dark green which can be readily observed. The experiments were designed carefully for the random selection of compositions of the samples. The dataset was randomly divided so that a part of it was used to train the model while the remaining part served as an independent test data set to measure the predictive ability of the model.

2.5. Spectral data collection

The redox couple mixtures were subjected to visible absorption spectroscopy for capturing the quantitative fingerprints of mixture

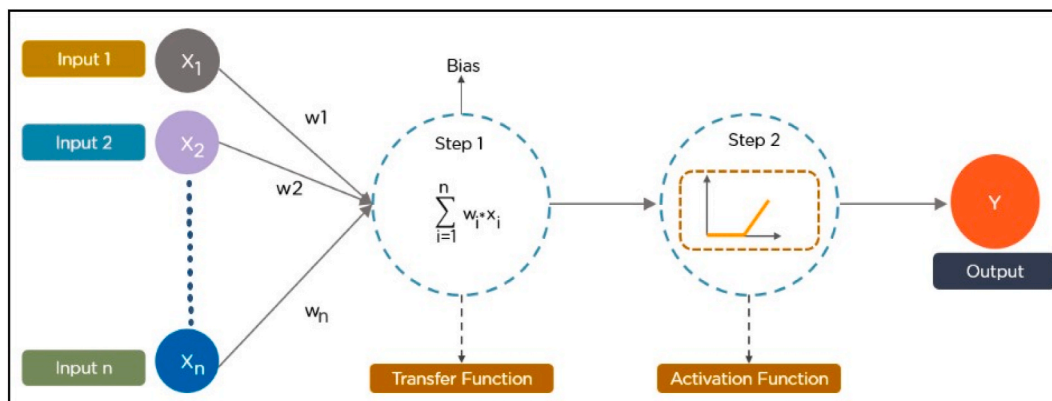


Fig. 1. General Architecture of an ANN model (Image source: [Superdatascience.com](https://www.superdatascience.com)).

composition. All spectral measurements were performed using the glacial acetic acid as a reference and readings were recorded in the visible range of 400–700 nm with a sampling interval of 1 nm on a medium scan rate, and a slit width of 2 mm. Each sample was scanned three times, and the average of three spectra was used to represent it. The spectral data was used without any pre-processing.

2.6. Reference wet analysis

The wet analysis of the samples was performed with iodometric titration using Sodium thiosulfate to obtain the concentration of Co (III) in each sample. This method, due to its simplicity, is one of the oldest preferred approaches for the routine analysis of a variety of chemical species including Co (III) [43]. It is usually done using starch as a visual indicator or an amperometric endpoint detection [44]. However, in the present study, an acetate buffer was used which eradicates the need for an external indicator. Co (II) amount was then calculated by the difference of total cobalt and Co (III).

2.7. Multivariate modelling

Application of Chemometrics and artificial intelligence to empirical modelling of spectral data is a promising method for multivariate calibration problems [32,45]. They have significantly improved and enhanced the scope of quantitative spectrophotometry and multiplied the importance of these methods by many folds in expanding analytical arenas. Multivariate modeling techniques such as partial least squares regression and artificial neural networks appear to be more adequate than univariate methods since they are proficient to handle complex mixtures and deal with negative effects of uncalibrated interferences and outliers existing in quantitative analysis [46].

Partial Least Square is a popular supervised learning method particularly known to be very effective among linear multivariate statistical methods. It is particularly admired in spectroscopy-related fields to deal with the problems of high dimensionality and multicollinearity of the variables. It maximizes the linear relationship between the concentration of the analyte and its spectra while minimizing the spectral interferences [27,33,47–50]. As compared to other linear methods like principal component regression, it takes into account the data of both spectra and concentration blocks to model the system and compute latent variable scores that achieve the greatest covariance between the matrix of independent variables X and the dependent variable y -vector. In the context of the present study the data matrix X is formed by UV-Visible spectra of the solution in the range of 400–700 nm and the y vector contains the experimental values for the concentration of Co (II) or Co (III) in the samples. PLS1 mode was applied in which the concentration of a single component is modelled at a time.

Artificial neural network (ANN) modeling is another very popular machine learning technique for developing nonlinear empirical models of complex chemical systems. ANN is now a mainstream technology mostly due to its excellent inherent ability to learn by examples without any human intervention. It recognizes the patterns in the input data and predicts the output of similar data sets. Due to its self-learning capacity and complexity solving, ANN has been implemented in various studies in diverse domains including chemical analysis [35,51].

Inspired by the conception of biological brains, ANN is composed of several artificial neurons that have adaptive and dynamic connections between them. ANN structures are mostly complex as a human brain and possess many other similar properties like self-learning, high parallelism, fault tolerance, and the ability to generalize and handle imprecise data.

ANN structures are usually multilayered as shown in Fig. 1. The input signals are received by the first layer, every input (x) is multiplied by an adjusted synaptic weight (W), then sum with bias (b) to form the net input (n). The net input (n) is passed through an activation function. The activation function is responsible for all complex computations in soft modelling mapping the input of a neural neuron to its output. Log sigmoid and linear transfer functions are the most common and make the model capable of good predictions. The neuron output (y) is written as:

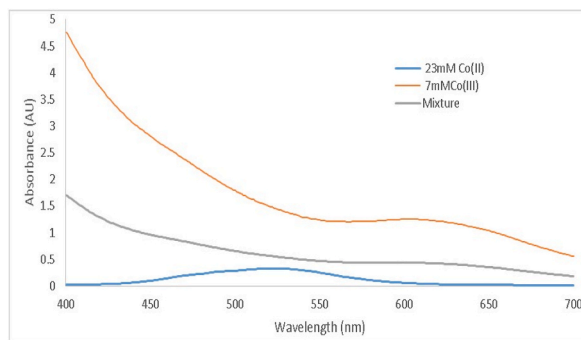


Fig. 2. Spectral overlap of standard solutions of Co (II) and Co (III) acetates and their binary mixture in water/acetic acid solution.

$$y = f(Wx + b)$$

The ability of ANN of universal approximation and recurrent dynamic modelling makes it very appealing to solve complex problems. However the model often requires a large training data set and the learning is computationally complex [36].

The details of PLS and ANN algorithms are present in several references [35,52] and therefore are not discussed here.

2.8. Internal and external validation of models

Several statistical parameters are used as figures of merit for model evaluation. A cross-validation procedure is a famous approach for internal validation during model training [52]. Leave –one out strategy is a common approach in which one sample is held out during training and its concentration is predicted by the trained model. The process is repeated until each sample is left out once and evaluation is done by Root mean square error of cross-validation, RMSECV or Predicted error sum of squares, PRESS for every component added or any topology change. After achieving an optimized model an independent test data set that was not used for model calibration is presented to the model and the concentration is predicted. The purpose of this independent test is to evaluate the reliability, extrapolation, and degree of prediction of the calibrated models. The root mean square error of calibration (RMSEC) and root mean square error of prediction (RMSEP) are the indicators used to assess the predictive ability of the model.

In addition to these error parameters, the correlation between predicted and experimental values is also taken into account by computing correlation coefficient R and coefficient of determination R^2 to judge the quality of prediction.

Errors of cross-validation and test set validation, bias, and the ratio of prediction to deviation (RPD) are calculated according to the following equations [27]:

Root mean square error of cross-validation (RMSECV):

$$RMSECV = \sqrt{\frac{\sum_{i=1}^N (\hat{C}_i - C_i)^2}{N}}$$

PRESS can be computed in the following manner:

$$PRESS = \sum_{i=1}^n (\hat{C}_i - C_i)^2$$

Coefficient of determination (R^2):

$$R^2 = 1 - \frac{\sum_{i=1}^N (\hat{C}_i - C_i)^2}{\sum_{i=1}^N (\bar{C}_i - C_i)^2}$$

Bias:

$$Bias = \frac{\sum_{i=1}^N (\hat{C}_i - C_i)}{N}$$

The ratio of prediction to deviation (RPD):

$$RPD = \frac{SD}{RMSEP}$$

where \hat{C}_i the predicted or estimated concentration in the i th sample,

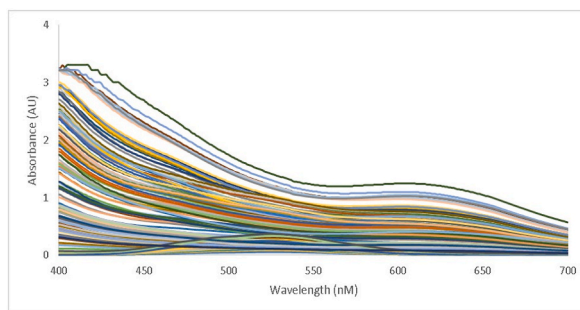


Fig. 3. The absorption spectra of 145 mixtures of Co (II) and Co (III) in acetic acid solution.

C_i is the actual/experimental value of the concentration in the sample,

\bar{C}_i is the mean of the experimental values,

N is the number of samples in the validation set,

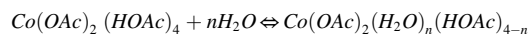
SD is the standard deviation.

3. Results and discussion

3.1. Spectral features

The spectral response of Co (II) and Co (III) present simultaneously in acetic acid solution is complicated due to their spectral overlap. It can be seen in Fig. 2, that these compounds don't show sharp peaks but rather broad peaks are observed in their solution.

Mostly industrially important oxidation reactions based on the Cobalt catalyst system are operated in a water/acetic acid ($H_2O/AcOH$) solvent system. Dissolution of transition metal compounds such as cobalt acetate in acetic acid/water mixtures results in significant changes in their coordination chemistry. Solution chemistry of cobalt acetate is complex as several octahedral and tetrahedral coordination complexes are formed through various equilibria steps, all of them dependent on the acid/water concentration ratio [7,53] In general, the equilibria of cobalt acetate with water in acetic acid may be written as follows:



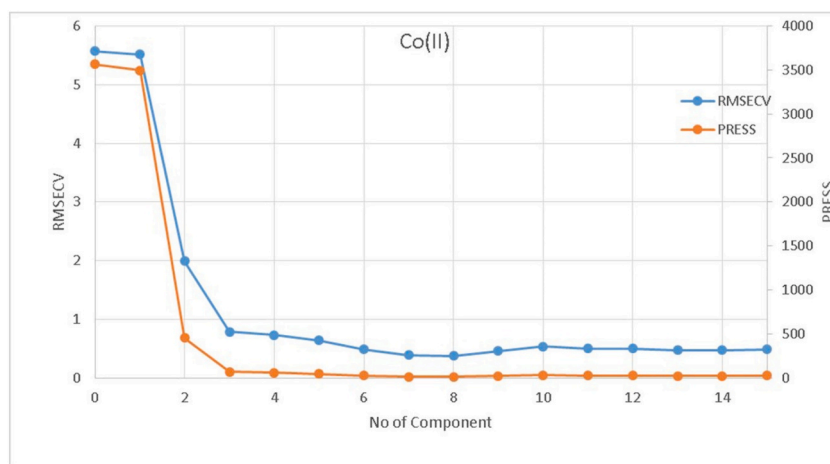
The stepwise formation constants for these species have been reported in the literature [54] and can be used to calculate their distribution. However, in the present study the concentration of Co(II) refers to the total amount of Co(II) species present in the solution. In the spectra of cobalt acetate (Fig. 2) a broad peak attributed to $Co(OAc)_2$ species is prominent, which is shifted from one wavelength to another (525 nm–515 nm) according to the composition of solvent and amount of water in it [49]. The active catalyst is prepared via one-electron oxidation of the metals by oxidants such as peroxy radicals or potassium chlorate as in the present case occurs. The resulting solution contains Co (III) acetate in addition to unreacted Co (II) species.

Studies show a shift of absorption maxima of Co (III) acetate from 600 nm to 585 nm in anhydrous acetic acid to water respectively at 25 °C [55]. Since the spectral feature is not of pure species rather it's a combined spectrum of several species, thus univariate spectroscopy couldn't be a good option for compositional analysis. The UV-vis spectra for samples of redox couple mixtures prepared at various Co (II) concentrations (0.06–23.0 mM) and Co(III) (0.02–6.5 mM) in varying $H_2O/AcOH$ ratios in the range of 400–700 nm are shown in Fig. 3, that provides complimentary information on the catalyst composition.

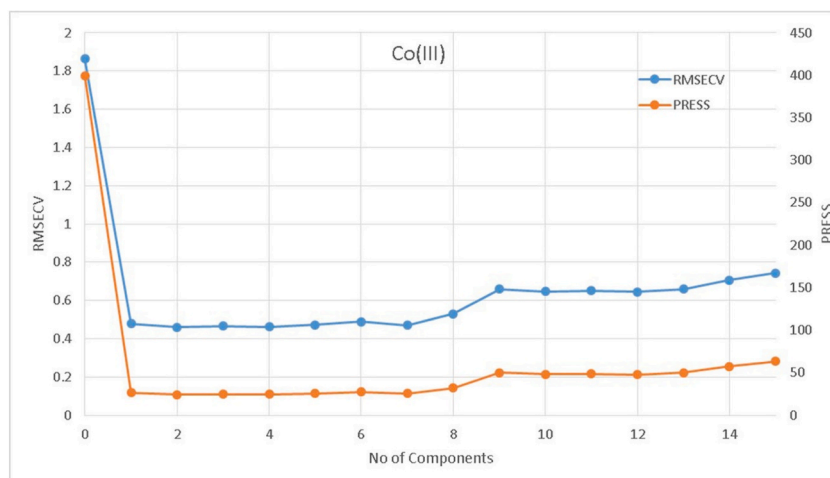
Chloride ions produced during the synthesis of the redox couple would not interfere much during the collection of visible absorption spectra as this specie doesn't contribute to spectra in this range. The same is true for some unreacted ClO_3^- ions and trace quantities of water added and produced during the synthesis of redox couple mixtures. The spectra are generally very similar in shape and thus have a high degree of correlation. To overcome this problem, two different multivariate calibration models are proposed and their results are compared.

3.2. PLS model

A PLS model was developed using the SIMPLS algorithm and the data were mean centered. 145 samples of binary mixtures of Co (II) and Co (III) were used to develop the model. In the first step of model calibration, A 115×301 X matrix consisting of absorbance of 115 samples on 301 wavelength points (400–700 nm) for PLS was used for calibration of the model. The experimentally found concentration of each component was provided separately as the Y matrix of 115×1 dimension. PLS-1 mode of regression was adopted in which each component is measured separately. A major task in model development is to select the appropriate number of factors or latent variables best representing the relationship between the spectra and analyte concentration. For this purpose, Cross-validation with leave one out strategy is the most common one. The number of factors selected for Co(II) and Co(III) are 3 and 2 respectively on the basis of RMSECV (or PRESS) as shown in Fig. 4(a and b). Up to these numbers of factors, the RMSECV (as well as PRESS) decreases sharply to 0.789 for Co (II) and 0.479 mM for Co (III) and then it nearly level off. The model was built with the selected number of



(a)



(b)

Fig. 4. RMSECV and PRESS versus the number of components for (a) Co (II) and (b) Co (III) in the PLS1 model.

latent variables and used to predict the concentration of another set of 30 samples that were not used previously in model development. The root mean square error of prediction was found to be 1.16 and 0.536 mM for Co (II) and Co (III). Moreover, the coefficients of determination for both calibration and validation show a reasonable prediction ability of the model for both components (See Figs. 5 and 6, Table 1). The results show good predictive ability of the PLS model for both components.

3.3. The ANN model

To model Co (II) and Co (III) concentrations and their spectra in acetic acid solution, the data matrix comprising of absorbance of 145 mixture on 301 wavelengths at a difference of 1 nm were added as an input data and the experimental concentrations of both Co (II) and Co (III) were added to the network toolbox separately as target matrices. As a common practice of ANN model training, 70% of the data was assigned for network training, 15% was used for network generalization while the remaining 15% was presented to the network as an unlearned test data to access the prediction ability of the model. The neural network architecture is a crucial parameter to decide model performance.

A multi-layered feed forward-back propagation (FFBP-NN) neural network with Levenberg –Marquardt (LM) algorithm for its fast convergence was developed. A three-layered artificial neural network program was written in Matlab. This model consisted of an input layer with 301 neurons corresponding to each wavelength's spectra. 10 neurons were selected for the hidden layer where all computations take place, ensuring good fitting of data. The output of the single neuron in the output layer corresponds to the modelled concentration of the component. The log sigmoid transfer function was used for hidden layers of this network and linear transfer

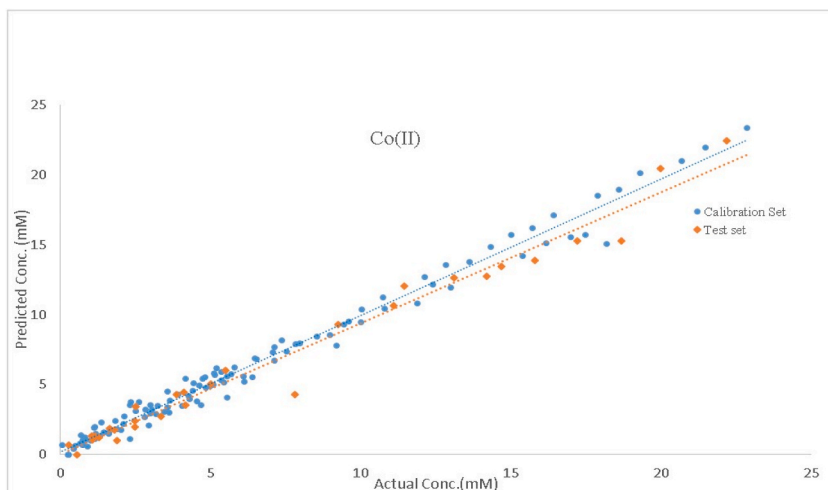


Fig. 5. Predicted concentration versus measured concentration for Co (II) in 115 Calibration sets and 30 Test sets.

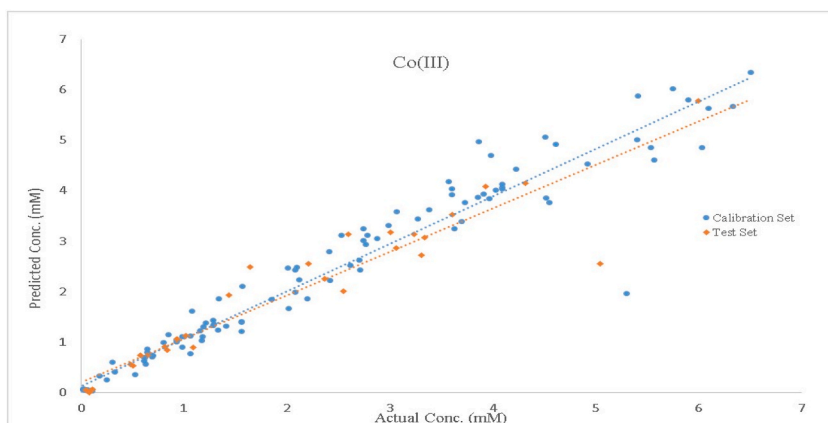


Fig. 6. Predicted concentration versus measured concentration for Co (III) in 115 Calibration sets and 30 Test sets.

Table 1

Statistics of the calibration and test set validation of the PLS-R models for estimating Co (II) and Co (III) in acetic acid solution based on original UV-Visible spectra.

Analyses	Number of independent variables	Model	LV	Calibration Set Validation (115 Samples)		Test Set Validation (30 Samples)		RDP	Bias (mM)
				R_C^2	RMSEC (mM)	R_p^2	RMSEP (mM)		
Co(II)	301	PLS	3	0.985	0.690	0.975	1.16	5.49	0.438
Co(III)	301	PLS	2	0.940	0.449	0.892	0.536	2.79	0.068

Abbreviations: LV, latent variables; R_C^2 , coefficient of determination for calibration; RMSEC, root mean square error for calibration; R_p^2 , coefficient of determination for prediction; RMSEP, root mean square error for prediction; RPD, the ratio of standard deviation to the standard error of prediction; Bias, average error of prediction.

function was used for the output layer. Models using sigmoid transfer functions often are capable to model complex and nonlinear systems with improved accuracy.

During the training phase, the network selects random values of weight and bias. This training was performed for each component separately with LM algorithms for error minimization, and after fine-tuning the model, RMSE for each component in every step has been displayed in Table 2. Also, the predicted concentrations are plotted against the actual concentrations in Figs. 7 and 8. A larger coefficient of determination (R^2) endorses the capability of better predictions of both components.

Table 2
Summary of performance parameters of the ANN model.

Analyses	Type of Algorithm	Number of Layers	No. of Neuron	Training (115 samples)		Validation (15 Samples)		Testing (15 Samples)	
				R ²	RMSE (mM)	R ²	RMSE (mM)	R ²	RMSE (mM)
Co(II)	LM	3	10	0.996	0.332	0.996	0.316	0.996	0.316
Co(III)	LM	3	10	0.956	0.374	0.968	0.300	0.988	0.346

LM = Levenberg-Marquardt; R² = Coefficient of determination; RMSE = Root mean square error.

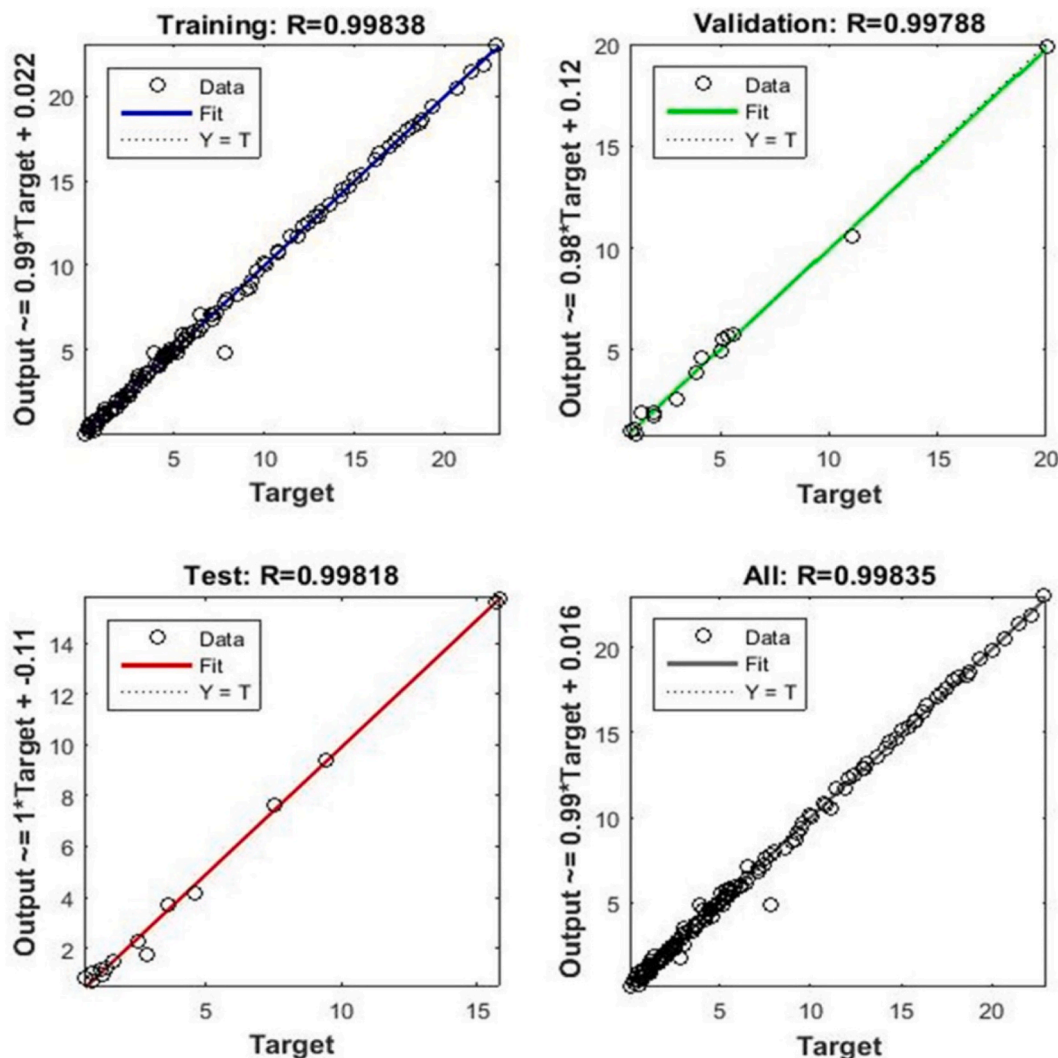


Fig. 7. Predicted concentrations versus the actual concentrations related to training, validation, and test series for Co (II) using the LM algorithm.

3.4. Comparison of models

The different figures of merit for both models show that they are capable of satisfactory prediction of both Co (II) and Co (III). The plots of the error histogram Fig. 9(a) and (b) show random variation without any systematic error present in the models. Similarly, random errors are observed in PLS models for both Co (II) and Co (III) (Fig. 10).

The p-values of PLS and ANN calibration models can be seen on the regression summary analysis table (Table 3). Both models are acceptable on this basis since p-values for slope and intercept are below the level of significance i. e, 0.05. However, p-values for the ANN model are well below the chosen significance level, almost zero in each case, as compared to the p-values for PLS model which are just below 0.05 for slope for Co (II) and Co (III). It also shows that ANN model is capable of better predictions than PLS model and is the

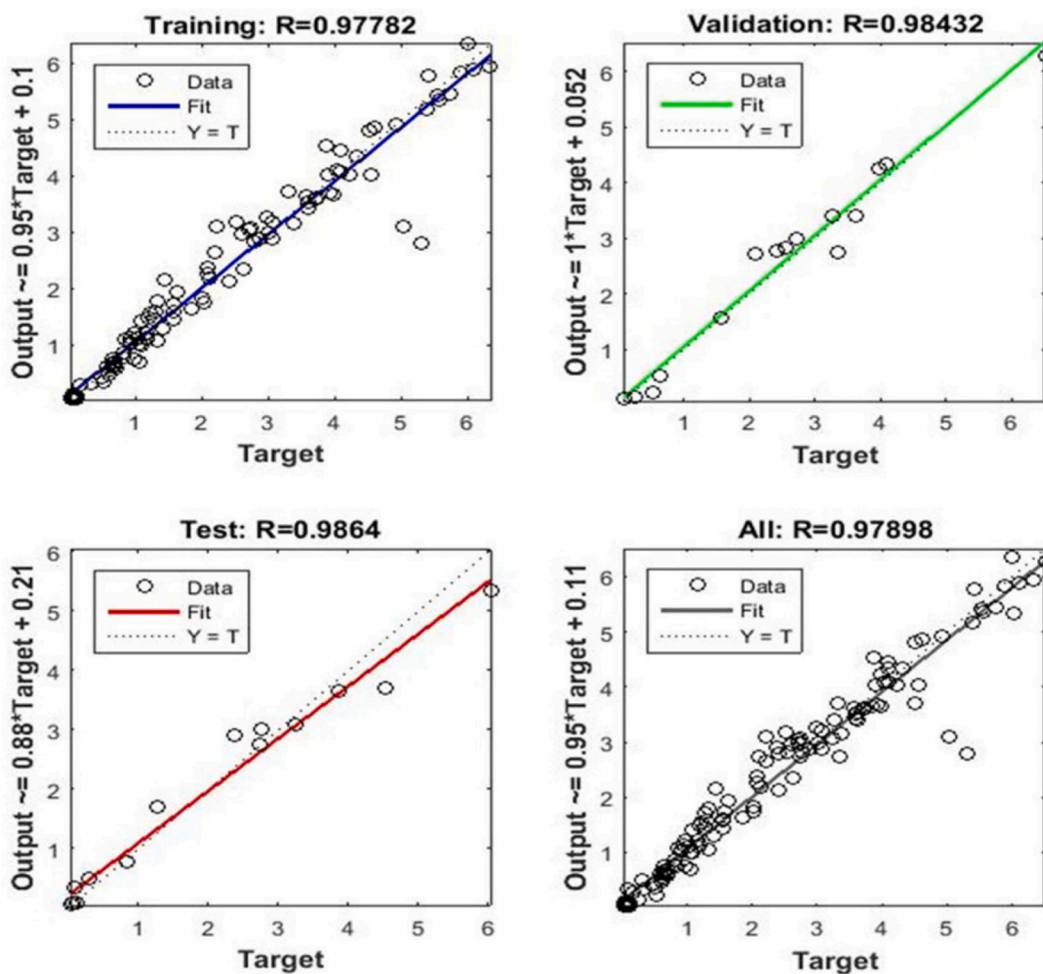


Fig. 8. Predicted concentrations versus the actual concentrations related to training, validation, and test series for Co (III) using the LM algorithm.

preferred choice for both Co (II) and Co (III).

The performance of each methods is also evaluated using the percentage recovery values (%RE) of the concentrations of both components. Results of %RE in Table 4 show that better recovery values are obtained for ANN model as compared to PLS.

In general ANN model is capable to outperform the PLS regression model not just from a performance point of view but also due to its self-learning ability and independent decision-making without requiring any experts' intervention. Its excellent generalization capacity for linear as well as nonlinear data trends is shown by the prediction excellence and better fitting for unlearned data.

4. Conclusion

Redox couple of cobalt Co (II)/Co (III) in acetic acid solution has particular importance in organic industrial processes. The inherent link between catalyst composition and reaction kinetics renders paramount importance to the elucidation of the catalyst composition. However, the accurate determination of the concentration of both Co (II) and Co (III) species simultaneously is quite challenging with conventional spectroscopy due to spectral overlap.

Chemometric and machine learning algorithm has now gained widespread acceptance in all fields and is especially popular in multivariate spectroscopic analysis of complex mixtures. Partial least squares regression and artificial neural network were used to model the relation between UV-Visible spectra and the molar concentration of both Co (II) and Co (III) species present simultaneously in the acetic acid solution.

A large data set was used to train and optimize the regression models with cross-validation. The predictive ability of the model was evaluated by an independent test set.

Statistical results render both models to be pertinent. The developed PLS and ANN models are capable of the robust compositional analysis of the catalyst solution, not just because of low mean square error values for prediction but also due to the high determination coefficient of the external validation of the model and satisfactory recovery values. The assessment of the results of internal and external validation of models revealed the ANN-based models to have a better performance than the PLS ones.

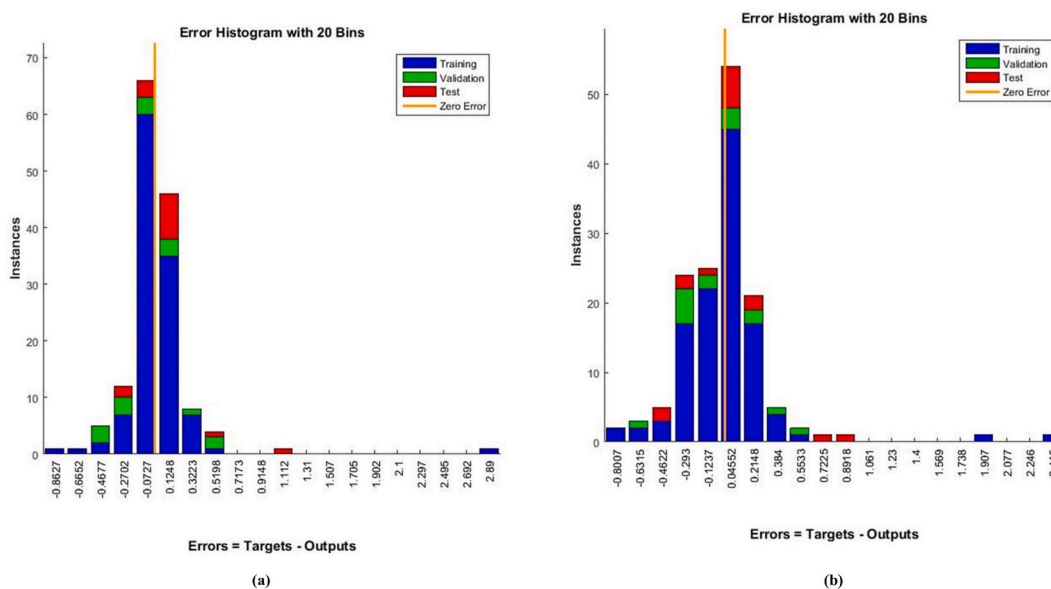


Fig. 9. Error histogram of (a) Co (II) and (b) Co (III) for ANN model.

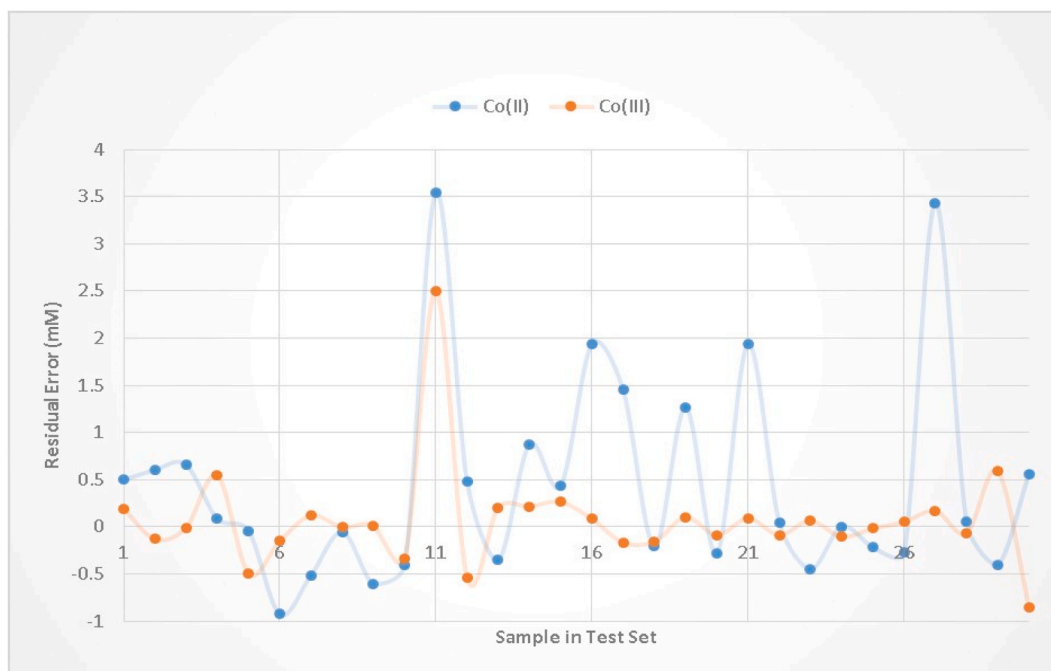


Fig. 10. The plot of residual error between the experimental and predicted concentration of Co (II) and Co (III) in a test set by PLS regression.

Data availability statement

Data will be made available on request.

CRedit authorship contribution statement

Nausheen Yasin: Conceptualization, Data curation, Formal analysis, Resources, Validation, Writing – original draft. **Syed Mumtaz Danish Naqvi:** Conceptualization, Methodology, Supervision, Writing – review & editing. **Syed Mamnoon Akhter:** Formal analysis, Software.

Table 3

Summary of regression analysis of the calibration models for 115 solutions of Co (II) and Co (III).

Specie	Chemometric technique	Parameter	Coefficients	Standard Error	t Stat	P-value
Co(II)	PLS	Intercept	0.190	9.63E-02	1.97	0.051
		Slope	0.975	1.15E-02	84.7	0.000
	ANN	Intercept	0.022	5.33E-16	4.13E+13	0.000
		Slope	0.990	6.37E-17	1.55E+16	0.000
Co(III)	PLS	Intercept	0.126	6.25E-02	2.01	0.046
		Slope	0.941	2.22E-02	42.3	0.000
	ANN	Intercept	0.100	1.11E-16	8.97E+14	0.000
		Slope	0.950	3.95E-17	2.40E+16	0.000

Note: level of significance = 0.05.

Table 4

Recoveries of Co (II) and Co (III) in 15 test samples by the calibration models.

Solution number	Co(II)					Co(III)				
	Actual value (mM)	Predicted value by PLS (mM)	RE (%)	Predicted value by ANN (mM)	RE (%)	Actual value (mM)	Predicted value by PLS (mM)	RE (%)	Predicted value by ANN (mM)	RE (%)
1	3.36	2.76	82.0	3.34	99.5	0.936	1.07	113.9	1.00	106.8
2	4.18	3.52	84.3	4.15	99.4	0.835	0.84	101.0	0.90	108.2
3	2.47	2.39	96.6	2.46	99.6	2.55	2.01	78.6	2.53	99.3
4	5.00	5.04	100.0	4.97	99.3	1.44	1.93	134.3	1.48	102.6
5	11.1	10.6	95.7	11.0	99.1	2.6	3.14	120.7	2.58	99.2
6	4.12	4.47	108.6	4.09	99.4	3.06	2.86	93.5	3.02	98.6
7	13.1	12.7	96.7	12.9	99.1	3.34	3.08	92.1	3.28	98.3
8	14.2	12.7	89.8	14.1	99.1	3.01	3.18	105.6	2.97	98.7
9	1.15	1.36	117.9	1.15	100.4	0.575	0.731	127.2	0.66	114.1
10	14.7	13.4	91.4	14.6	99.1	3.24	3.14	96.9	3.19	98.4
11	15.8	13.8	87.7	15.7	99.1	3.61	3.52	97.5	3.54	98.0
12	1.29	1.25	96.7	1.29	100.2	0.646	0.73	113.5	0.72	112.0
13	1.06	1.06	100.1	1.07	100.5	1.02	1.13	110.3	1.08	105.8
14	18.7	15.3	81.7	18.5	99.1	4.32	4.15	96.1	4.21	97.5
15	1.81	1.76	97.1	1.81	99.9	0.485	0.553	114.0	0.57	117.7

Abbreviations: PLS, Partial Least Square; ANN, Artificial Neural Network; RE, Percent recovery.

Declaration of competing interest

The authors declare that they have no known competing financial interests or personal relationships that could have appeared to influence the work reported in this paper.

References

- [1] A. Ward, A. Masters, T. Maschmeyer, Cobalt(II) Carboxylate Chemistry and Catalytic Applications, 2013, pp. 665–684, <https://doi.org/10.1016/B978-0-08-097774-4.00630-6>.
- [2] S.M.D. Naqvi, et al., Selective Homogeneous Oxidation System for Producing Hydroperoxides Concentrate: Kinetic Simulation of Catalytic Oxidation of Gas Oils, vol. 49, 2010, pp. 7210–7226, <https://doi.org/10.1021/ie100327m>, 16.
- [3] D.J. Cole-Hamilton, Homogeneous Catalysis—New Approaches to Catalyst Separation, Recovery, and Recycling, vol. 299, 2003, pp. 1702–1706, <https://doi.org/10.1126/science.1081881>, 5613.
- [4] Q. Lyu, et al., Modeling of the Co-Mn-Br Catalyzed Liquid Phase Oxidation of p-Xylene to Terephthalic Acid and m-Xylene to Isophthalic Acid, vol. 232, 2021, 116340, <https://doi.org/10.1016/j.ces.2020.116340>.
- [5] S.M.D. Naqvi, et al., Liquid-Phase Homogeneous Catalytic Oxidation of Gas Oil: Elucidation of Complex Chemical Transformation Network, vol. 11, 2015, pp. 136–142, <https://doi.org/10.6000/1927-5129.2015.11.19>.
- [6] X. Liu, et al., Thermodynamic Analysis of Ammoniacal Thiosulphate Leaching of Gold Catalysed by Co (III)/Co (II) Using Eh-pH and Speciation Diagrams, vol. 178, 2018, pp. 240–249, <https://doi.org/10.1016/j.hydromet.2018.05.014>.
- [7] R.L. Taylor, et al., The Influence of Solvent Composition on the Coordination Environment of the Co/Mn/Br Based Para-Xylene Oxidation Catalyst as Revealed by EPR and ESEEM Spectroscopy, 2022, <https://doi.org/10.1039/D2CY00496H>.
- [8] J.C. Chang, et al., Determination of cobalt in cobalt (III) complexes-A comparative study, in: Proceedings of the Iowa Academy of Science, 1980.
- [9] J.E. Hicks, The separation and determination of Cobalt (II) and Cobalt (III), J. Anal. Chim. Acta 45 (1) (1969) 101–108.
- [10] K. Ravindranath, M. Subbaiyan, Chemical Sciences, Paper chromatographic separation of cobalt (II) and cobalt (III) via their acetylacetonate complexes, J.P.o. t.I.A.o.S.-S.A. 87 (12) (1978) 461–463, <https://doi.org/10.1007/BF03182165>.
- [11] K. Ravindranath, P. Janardhan, Thin-layer chromatographic separation of cobalt (II) and cobalt (III) via their acetylacetonates, JCS (J. Chromatogr. Sci.) (1986) 232–234.
- [12] J.R. Chipperfield, S. Lau, D.E. Webster, Speciation in cobalt(III)-catalysed autoxidation: studies using thin-layer chromatography, J. Mol. Catal. 75 (2) (1992) 123–128, [https://doi.org/10.1016/0304-5102\(92\)80113-U](https://doi.org/10.1016/0304-5102(92)80113-U).
- [13] K. Matsumoto, et al., Application of TLC-MALDI-TOFMS to Identification of Co (II) and Co (III) Acetylacetonates, vol. 50, 2002, pp. 15–17, 1.
- [14] J.I. Watters, I.M. Kolthoff, Polarographic procedure for determination of cobalt as cobalt(III) ammine, Anal. Chem. 21 (12) (1949) 1466–1469.

- [15] E. Beinrohr, Spectrophotometric determination of cobalt(II) and cobalt(III) after separation in ammonia solution by precipitating cobalt(II) with acetylacetone, *Analyst* 110 (11) (1985) 1317–1320, <https://doi.org/10.1039/AN9851001317>.
- [16] M.J. Ahmed, K.J. Hossain, A rapid spectrophotometric method for the determination of cobalt in industrial, environmental, biological, pharmaceutical and soil samples using bis (5-bromosalicylaldehyde) orthophenylenediamine, *J.J.o.t.I.C.S.* 5 (4) (2008), <https://doi.org/10.1007/BF03246149>.
- [17] S. Chandramouleeswaran, J. Ramkumar, Speciation studies of cobalt (II) and cobalt (III) and its application to sample analysis, *J.L.J.o.A.i.C.S.* 2 (2) (2014) 134–139.
- [18] T. Stafilov, Determination of trace elements in minerals by electrothermal atomic absorption spectrometry, *J.S.A.P.B.A.S.* 55 (7) (2000) 893–906, [https://doi.org/10.1016/S0584-8547\(00\)00227-5](https://doi.org/10.1016/S0584-8547(00)00227-5).
- [19] A.T. Weakley, et al., Quantifying Silica in Filter-Deposited Mine Dusts Using Infrared Spectra and Partial Least Squares Regression, vol. 406, 2014, pp. 4715–4724, <https://doi.org/10.1007/s00216-014-7856-y>, 19.
- [20] A.L. Miller, et al., Direct-on-filter α -quartz Estimation in Respirable Coal Mine Dust Using Transmission Fourier Transform Infrared Spectrometry and Partial Least Squares Regression, vol. 71, 2017, pp. 1014–1024, <https://doi.org/10.1177/0003702816666288>, 5.
- [21] C.A. Duran-Villalobos, et al., Multivariate Statistical Data Analysis of Cell-free Protein Synthesis toward Monitoring and Control, vol. 67, 2021 e17257, <https://doi.org/10.1002/aic.17257>, 6.
- [22] Y. Wang, et al., Kinetic Study of Product Distribution Using Various Data-Driven and Statistical Models for Fischer–Tropsch Synthesis, vol. 6, 2021, pp. 27183–27199, <https://doi.org/10.1021/acsomega.1c03851>, 41.
- [23] C.L. Cunha, A.R. Torres, A.S. Luna, Multivariate regression models obtained from near-infrared spectroscopy data for prediction of the physical properties of biodiesel and its blends, *J.F.* 261 (2020) 116344, <https://doi.org/10.1016/j.fuel.2019.116344>.
- [24] E. Wikberg, et al., Calibration Method for the Determination of the FAME and HVO Contents in Fossil Diesel Blends Using NIR Spectroscopy, vol. 2, 2021, pp. 179–193, <https://doi.org/10.3390/fuels2020011>, 2.
- [25] C.d.S. Araújo, et al., Determination of pH and Acidity in Green Coffee Using Near-infrared Spectroscopy and Multivariate Regression, vol. 100, 2020, pp. 2488–2493, <https://doi.org/10.1002/jsfa.10270>, 6.
- [26] O. Uncu, B. Ozen, F. Tokatli, Use of FTIR and UV–visible spectroscopy in determination of chemical characteristics of olive oils, *Talanta* 201 (2019) 65–73, <https://doi.org/10.1016/j.talanta.2019.03.116>.
- [27] W. Zhou, et al., A Rapid Analytical Method for the Quantitative Determination of the Sugar in Acarbose Fermentation by Infrared Spectroscopy and Chemometrics, vol. 240, 2020 118571, <https://doi.org/10.1016/j.saa.2020.118571>.
- [28] A. Puliyaanda, et al., A Review of Automated and Data-Driven Approaches for Pathway Determination and Reaction Monitoring in Complex Chemical Systems, 2021 100009, <https://doi.org/10.1016/j.dche.2021.100009>.
- [29] K. Sivaramakrishnan, et al., A Data-Driven Approach to Generate Pseudo-reaction Sequences for the Thermal Conversion of Athabasca Bitumen, vol. 6, 2021, pp. 505–537, <https://doi.org/10.1039/D0RE00321B>, 3.
- [30] M. Aljunaid, Y. Tao, H. Shi, A novel mutual information and partial least squares approach for quality-related and quality-unrelated fault detection, *J.P.* 9 (1) (2021) 166, <https://doi.org/10.3390/pr9010166>.
- [31] H. Zhang, Q. Zhu, Concurrent multilayer fault monitoring with nonlinear latent variable regression, *Ind. Eng. Chem. Res.* 61 (3) (2022) 1423–1442, <https://doi.org/10.1021/acs.iecr.1c03360>.
- [32] M. Driouch, et al., Development and Validation of QSPR Models for Corrosion Inhibition of Carbon Steel by Some Pyridazine Derivatives in Acidic Medium, vol. 6, 2020, <https://doi.org/10.1016/j.heliyon.2020.e05067>, 10.
- [33] V. Arabzadeh, M.R. Sohrabi, Artificial neural network and multivariate calibration methods assisted UV spectrophotometric technique for the simultaneous determination of metformin and Pioglitazone in anti-diabetic tablet dosage form, *J.C. and I.L. Systems* 221 (2022) 104475, <https://doi.org/10.1016/j.chemolab.2021.104475>.
- [34] P. Barmpalexis, et al., Artificial Neural Networks (ANNs) and Partial Least Squares (PLS) Regression in the Quantitative Analysis of Cocrystal Formulations by Raman and ATR-FTIR Spectroscopy, vol. 158, 2018, pp. 214–224, <https://doi.org/10.1016/j.jpba.2018.06.004>.
- [35] M. Salehi, et al., Artificial Neural Networks (ANNs) and Partial Least Squares (PLS) Regression in the Quantitative Analysis of Respirable Crystalline Silica by Fourier-Transform Infrared Spectroscopy (FTIR), vol. 65, 2021, pp. 346–357, <https://doi.org/10.1016/j.jpba.2018.06.004>, 3.
- [36] A. Tahir, et al., Neural Network and Regression Methods for Estimation of the Average Daily Temperature of Hyderabad for the Years 2018–2020, vol. 12, 2021, pp. 87–91, <https://doi.org/10.46660/ijeeg.v12i2.107>, 2.
- [37] N. Sarlak, M. Anizadeh, Simultaneous kinetic spectrophotometric determination of sulfide and sulfite ions by using an optode and the partial least squares (PLS) regression, *J.S. A.B. Chem.* 160 (1) (2011) 644–649, <https://doi.org/10.1016/j.snb.2011.08.042>.
- [38] A. Niazi, Simultaneous spectrophotometric determination of FeII and FeIII in pharmaceuticals by partial least squares with chromogenic mixed reagents, *J.C.c.a.* 79 (4) (2006) 573–579.
- [39] S. Khani, et al., Using the Extract of Pomegranate Peel as a Natural Indicator for Colorimetric Detection and Simultaneous Determination of Fe³⁺ and Fe²⁺ by Partial Least Squares–Artificial Neural Network, vol. 37, 2023, p. e3390, <https://doi.org/10.1002/cem.3390>, 1.
- [40] A. Safavi, H. Abdollahi, M.R. Hormozi Nezhad, Artificial neural networks for simultaneous spectrophotometric differential kinetic determination of Co(II) and V (IV), *Talanta* 59 (3) (2003) 515–523, [https://doi.org/10.1016/S0039-9140\(02\)00542-8](https://doi.org/10.1016/S0039-9140(02)00542-8).
- [41] L. Hejazi, et al., Solid-phase Extraction and Simultaneous Spectrophotometric Determination of Trace Amounts of Co, Ni and Cu Using Partial Least Squares Regression, vol. 62, 2004, pp. 183–189, [https://doi.org/10.1016/S0039-9140\(03\)00412-0](https://doi.org/10.1016/S0039-9140(03)00412-0), 1.
- [42] S.M.D. Naqvi, F. Khan, Selective homogeneous oxidation system for producing hydroperoxides concentrate: kinetics of catalytic oxidation of gas oils, *J.I. E.C. Res.* 48 (12) (2009) 5642–5655, <https://doi.org/10.1021/ie900364w>.
- [43] H. Laitinen, L. Burdett, Iodometric determination of cobalt, *J.A.C.* 23 (9) (1951) 1268–1270.
- [44] A. Guvenc, B. Karabacakoglu, Study of the effect of number of layers on the electrosynthesis of cobalt (III) acetate in a bipolar packed-bed flow reactor, *J.T.J.o.C.* 25 (4) (2001) 461–468.
- [45] M.N. Pervez, et al., Sustainable Fashion: Design of the Experiment Assisted Machine Learning for the Environmental-Friendly Resin Finishing of Cotton Fabric, vol. 9, 2023, <https://doi.org/10.1016/j.heliyon.2023.e12883>, 1.
- [46] R. Bro, Multivariate calibration: what is in chemometrics for the analytical chemist? *Anal. Chim. Acta* 500 (1) (2003) 185–194, [https://doi.org/10.1016/S0003-2670\(03\)00681-0](https://doi.org/10.1016/S0003-2670(03)00681-0).
- [47] A.R. Coscione, et al., Multivariate Calibration Applied to a Highly Interfering Chemical System: the Simultaneous Spectrophotometric Determination of Aluminium and Iron in Plants Using Xylenol Orange and Partial Least-Squares Regression, vol. 423, 2000, pp. 31–40, [https://doi.org/10.1016/S0003-2670\(00\)01102-8](https://doi.org/10.1016/S0003-2670(00)01102-8), 1.
- [48] Y. Ni, C. Huang, S. Kokot, Simultaneous determination of iron and aluminium by differential kinetic spectrophotometric method and chemometrics, *Anal. Chim. Acta* 599 (2) (2007) 209–218, <https://doi.org/10.1016/j.aca.2007.08.005>.
- [49] Y.S. Al-Degs, J.A. Sweileh, Simultaneous determination of five commercial cationic dyes in stream waters using diatomite solid-phase extractant and multivariate calibration, *A.J.o.C.* 5 (2) (2012) 219–224, <https://doi.org/10.1016/j.arabjc.2010.08.016>.
- [50] H. Khajehsharifi, et al., The Comparison of Partial Least Squares and Principal Component Regression in Simultaneous Spectrophotometric Determination of Ascorbic Acid, Dopamine and Uric Acid in Real Samples, vol. 10, 2017, pp. S3451–S3458, <https://doi.org/10.1016/j.arabjc.2014.02.006>.
- [51] J.L.S. Fagundes, et al., A new method of developing ANN-isotherm hybrid models for the determination of thermodynamic parameters in the adsorption of ions Ag⁺, Co²⁺ and Cu²⁺ onto zeolites ZSM-5, HY, and 4A, *J. Environ. Chem. Eng.* 9 (5) (2021) 106126, <https://doi.org/10.1016/j.jece.2021.106126>.
- [52] R.G. Brereton, *Chemometrics: Data Analysis for the Laboratory and Chemical Plant*, John Wiley & Sons, 2003.

- [53] W. Partenheimer, The structure of metal/bromide catalysts in acetic acid/water mixtures and its significance in autoxidation, *J.J.o.M.C.A.-c.* 174 (2001) 29–33, [https://doi.org/10.1016/S1381-1169\(01\)00169-8](https://doi.org/10.1016/S1381-1169(01)00169-8).
- [54] F.A. Cotton, et al., *Advanced Inorganic Chemistry*, John Wiley and Sons, Inc, 1999.
- [55] C.F. Hendriks, et al., *The Structure of Cobalt (II) Acetate and Cobalt (III) Acetate in Acetic Acid Solution*, vol. 18, 1979, pp. 43–46, 1.